Received: 28 January 2022 | Accepted: 7 February 2022

DOI: 10.1111/mpp.13199

Molecular Plant Pathology WILEY

ORIGINAL ARTICLE

Identification of novel virulence factors in *Erwinia amylovora* through temporal transcriptomic analysis of infected apple flowers under field conditions

Jeffrey K. Schachterle[1,2] | Kristi Gdanetz[2] | Ishani Pandya[2] | George W. Sundin[1,2]

[1]Genetics and Genome Sciences Program, Michigan State University, East Lansing, MI, USA

[2]Department of Plant, Soil, and Microbial Sciences, Michigan State University, East Lansing, MI, USA

Correspondence
George W. Sundin, Genetics and Genome Sciences Program, Michigan State University, East Lansing, MI, USA.
Email: sundin@msu.edu

Present address
Jeffrey K. Schachterle, USDA, ARS, Cereal Crops Research Unit, Fargo, ND, USA

Funding information
National Institute of Food and Agriculture, Grant/Award Number: 2015-67013-23068; Michigan State University AgBioResearch; Michigan State University Project GREEEN

Abstract

The enterobacterial pathogen *Erwinia amylovora* uses multiple virulence-associated traits to cause fire blight, a devastating disease of apple and pear trees. Many virulence-associated phenotypes have been studied that are critical for virulence and pathogenicity. Despite the in vitro testing that has revealed how these systems are transcriptionally regulated, information on when and where in infected tissues these genes are being expressed is lacking. Here, we used a high-throughput sequencing approach to characterize the transcriptome of *E. amylovora* during disease progression on apple flowers under field infection conditions. We report that type III secretion system genes and flagellar genes are strongly co-expressed. Likewise, genes involved in biosynthesis of the exopolysaccharide amylovoran and sorbitol utilization had similar expression patterns. We further identified a group of 16 genes whose expression is increased and maintained at high levels throughout disease progression across time and tissues. We chose five of these genes for mutational analysis and observed that deletion mutants lacking these genes all display reduced symptom development on apple shoots. Furthermore, these induced genes were over-represented for genes involved in sulphur metabolism and cycling, suggesting the possibility of an important role for maintenance of oxidative homeostasis during apple flower infection.

KEYWORDS
dsbA, fire blight, flower transcriptome, *iscS*, *tpx*, virulence expression

1 | INTRODUCTION

Progression of fire blight disease of apple and pear trees requires the causative agent *Erwinia amylovora* to coordinately express virulence traits and spread through host tissues (Piqué et al., 2015; Zhao et al., 2005). During infection, *E. amylovora* cells encounter several differing and hostile environments presented by specific host cell and tissue types that present distinct physical and biochemical challenges. Precise expression of genes involved in overcoming host defences and barriers under appropriate conditions leads to successful infection for *E. amylovora*.

Multiple specific virulence factors are important for successful infection of apple and pear trees by *E. amylovora* (Kharadi et al., 2021), including flagellar motility (Bayot & Ries, 1986; Raymundo & Ries, 1980), production of exopolysaccharides (Bellemann et al., 1994; Geider, 2000; Geier & Geider, 1993; Gross et al., 1992; Nimtz et al., 1996), biofilm formation (Koczan et al., 2009, 2011), catalase activity (Santander et al., 2018), and the type III secretion system

(T3SS; Baker et al., 1993; Barny, 1995; Wei et al., 1992). When *E. amylovora* cells are deposited on the stigma of an apple flower, populations grow to densities of 10^6 to 10^7 colony-forming units (cfu) on and between papillae cells (Malnoy et al., 2012; Pusey, 2000; Slack et al., 2022). Moisture from rain or dew enables the bacterial cells to migrate down to the nectaries, where they use flagella to swim through nectar to reach natural openings in the hypanthium (Bayot & Ries, 1986). On invasion at the base of the floral cup, *E. amylovora* cells must use the T3SS to suppress host defences and initiate pathogenesis (Bogdanove et al., 1998). During leaf infection at shoot tips, *E. amylovora* cells will also invade vascular tissues and produce the exopolysaccharides amylovoran, levan, and cellulose to structurally promote biofilm formation and population growth (Castiblanco & Sundin, 2018; Koczan et al., 2009, 2011). From all infected tissues during the disease cycle, sufficient internal populations will emerge in ooze droplets, ready to be disseminated to new hosts (Slack et al., 2017). In addition to these virulence traits that are important for navigation of and survival in host tissues, the bacteria must also be able to appropriately acquire and utilize the nutrients that are available in the occupied environment. Studies have found that iron acquisition via siderophores (Dellagi et al., 1998) as well as nutrient acquisition and metabolism are essential for full virulence (Ramos et al., 2014).

Although several studies have been conducted to understand *E. amylovora* transcriptional regulatory networks using in vitro growth conditions (Ancona et al., 2016; Li et al., 2014; McNally et al., 2012; Wang et al., 2009), studies of gene expression during infection are limited. Expression of T3SS genes was assessed by reverse transcription quantitative real-time PCR (RT-qPCR) during infection of apple flowers, and it was found that these genes were rapidly induced, and expression peaked between 24 and 48 h postinoculation (hpi) (Pester et al., 2012). A recent study conducted transcriptomic analysis of *E. amylovora* in shoots of two apple cultivars, one with low susceptibility and the other highly susceptible (Puławska et al., 2017). This study found that the greatest difference in virulence gene expression was manifest at 24 hpi, but little difference between cultivars was observed at 6 days postinoculation (dpi). Another study used an in vivo expression technology (IVET) approach to identify genes rapidly induced on inoculation to immature pears (Zhao et al., 2005). This approach identified novel virulence factors important for disease progression in this model. These studies provide a foundation on which further experiments can build to provide a transcriptome level view of *E. amylovora* virulence trait expression.

While these in vivo expression studies provide important groundwork, the studies were conducted under controlled greenhouse (Pester et al., 2012; Puławska et al., 2017) or laboratory conditions (Zhao et al., 2005). In this study, we inoculated a native strain of *E. amylovora* to apple flowers on trees in a research orchard, and analysed *E. amylovora* gene expression at the transcriptome level. Because of the complexity of different host tissues and environments, rather than sample whole flowers we sampled and sequenced RNA from the stigma, flower base, or pedicel of inoculated flowers at four sampling time points postinoculation. Our sequencing results matched previously reported expression patterns (Pester et al., 2012) for T3SS genes. We furthermore confirmed several hypothesized gene expression patterns across time as infection progressed. We identified novel genes induced on inoculation and chromosomal deletion of these genes resulted in reduced virulence. Our results suggest an important role for sulphur cycling, metabolism, and oxidative state during fire blight disease progression on flowers.

2 | RESULTS

2.1 | Sequencing and gene expression

Our RNA sequencing of infected flowers resulted in a total of 424.5 million reads across all samples. The attempt to deplete plant-derived ribosomal and poly(A) transcripts was only moderately successful at early time points. In samples from apple flower stigmas at 12 hpi, only 0.1% of sequenced reads mapped to the *E. amylovora* ATCC 49946 genome (Figure S1). By 48 hpi, 1% of sequenced reads successfully mapped to the *E. amylovora* genome, and at 96 hpi, about 30% of sequenced reads mapped to the *E. amylovora* genome. Pure inoculum was used as evidenced by 98% of sequenced reads from the inoculum mapping to the *E. amylovora* genome. Principal component analysis of all biological replicates showed that all in planta samples separated clearly from inoculum samples and replicates clustered by tissue and time point (Figure 1a). Similarly, Pearson's correlation coefficients were high between biological replicates and hierarchical clustering also showed that replicates clustered by tissue and time point (data not shown).

Because of the low *E. amylovora* read counts at early time points, we were unable to determine differentially expressed genes using traditional analysis, but we were able to do so for later sampling time points. We generated a heat map across all sample replicates using the 394 genes differentially expressed between pedicel 96 hpi samples and the source inoculum (Figure 1b). We found that in our data set a majority of the differentially expressed genes were down-regulated during flower infection, represented as group II in Figure 1b. Among the genes with greatest decrease in expression in flower pedicels were a sugar efflux transporter, *setA*, and several putative two-component signalling system proteins. Because of the low sequencing depth in the inoculated flower samples, this group of down-regulated genes may have biological relevance, but also could be an artefactual observation, and further experimentation is needed to resolve this possibility. However, there are many genes with low expression levels in the inoculum (growth in Luria-Bertani [LB] medium) that increased at some point during flower infection, represented as group I in Figure 1b. The genes with the greatest increases in expression levels were primarily flagellar and T3SS genes. We selected 10 genes and conducted RT-qPCR from independent RNA samples to validate the expression levels observed in our RNA sequencing (RNA-Seq) experiments and found similar expression patterns between RNA-Seq and RT-qPCR (Figure S2).

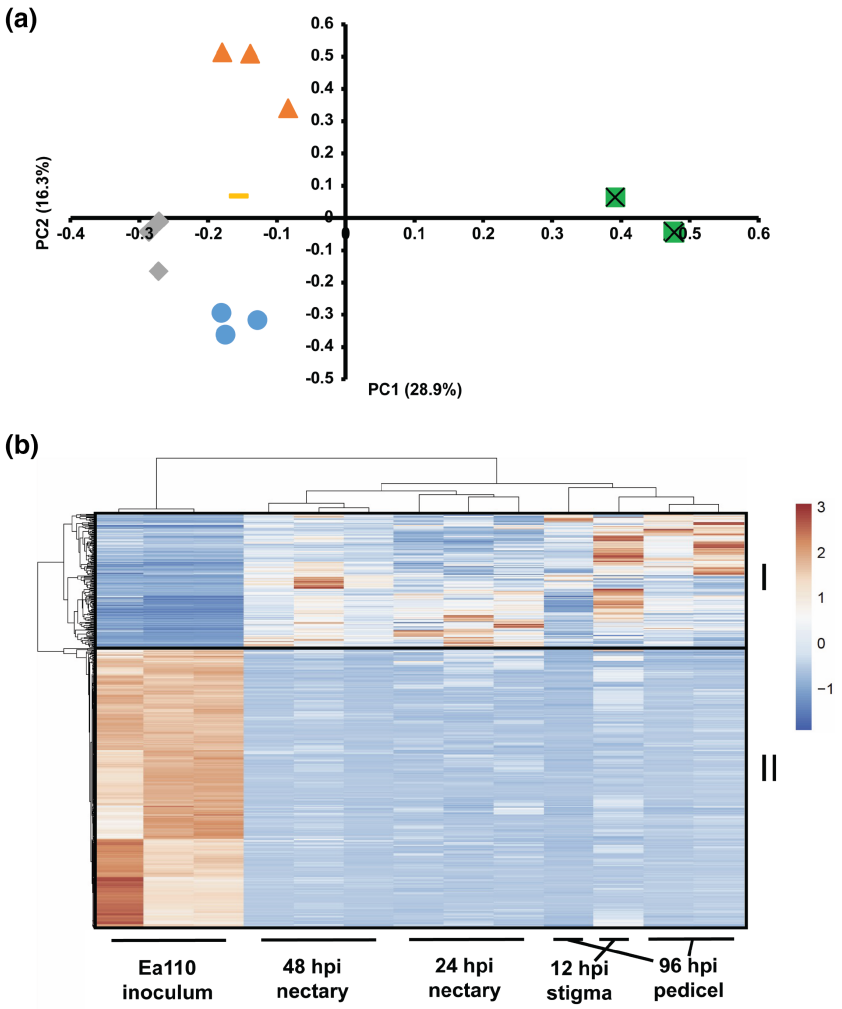

FIGURE 1 Multidimensional analysis of gene expression during infection under field conditions. (a) Principal component plot demonstrating clustering by tissue and time point. Squares represent *Erwinia amylovora* strain Ea110 grown in Luria-Bertani (LB) medium (inoculum); dash, 12 h stigma sample; circles, 24 h nectary samples; diamonds, 48 h nectary samples; triangles, 96 h pedicel samples. (b) Heat map of genes differentially regulated between cells grown in LB medium (inoculum) and cells in 96 h postinoculation (hpi) pedicel samples. Hierarchical clustering of genes divided genes into two broad groups, designated I and II, based on whether the gene of interest had increased or decreased mRNA abundance in inoculated samples compared to inoculum

2.2 | T3SS and *hrpL* gene expression profile

Because expression patterns for some T3SS genes were previously determined during flower infection (Pester et al., 2012), we analysed the expression patterns for all T3SS genes in our sequencing data set. We found that our results mirrored those previously found using RT-qPCR approaches, in which T3SS genes are rapidly induced on flower inoculation and expression starts to diminish as disease progresses to later stages (Figure 2a,b). Also, we found that the average induction of T3SS genes was about 10 times greater than that of the alternative sigma factor, *hrpL*, which is essential for expression of T3SS genes. This is consistent with the role of HrpL as a transcriptional regulator that is capable of signal amplification.

2.3 | Flagellar gene expression profiles

Similar to T3SS genes, we found that expression of flagellar genes was also rapidly and strongly induced on inoculation on flowers. Like the expression of T3SS genes, we found that expression of flagellar genes began to diminish at 96 hpi in the pedicel (Figure 2c). Although T3SS genes are organized in a single cluster in the genome, the flagellar genes of *E. amylovora* are spread across six gene clusters in the genome. Some of these clusters represent duplications of several flagellar genes (Koczan et al., 2011). By separating the average expression level of each flagellar cluster individually, we see that flagellar clusters 1 (EAM_1436–EAM_1449; ATCC 49946 genome), 2 (EAM_1484–EAM_1498), and 4 (EAM_2062–EAM_2071) showed increased expression during flower infection, but clusters 3 (EAM_2019–EAM_2034), 5 (EAM_2537–EAM_2561), and 6 (EAM_2568–EAM_2588) only showed small changes in expression throughout infection (Figure 2d). Interestingly, flagellar clusters 5 and 6 are duplicates of clusters 2 and 3, respectively, and are not involved in flagellar motility (Zhao et al., 2010) but may have roles in surface attachment (Koczan et al., 2011).

Because it has been reported that flagellar and T3SS genes are co-expressed during shoot infection (Puławska et al., 2017), we conducted a linear regression to test for correlation between expression of the T3SS genes and each of the flagellar gene clusters (Figure S3). We found that expression of flagellar cluster 1 had the strongest correlation to T3SS expression ($R^2 = 0.588$), and that clusters 2 and 4 had weak correlations ($R^2 = 0.338$ and $R^2 = 0.109$, respectively). In addition, flagellar clusters 3, 5, and 6 had essentially no correlation ($R^2 < 0.05$).

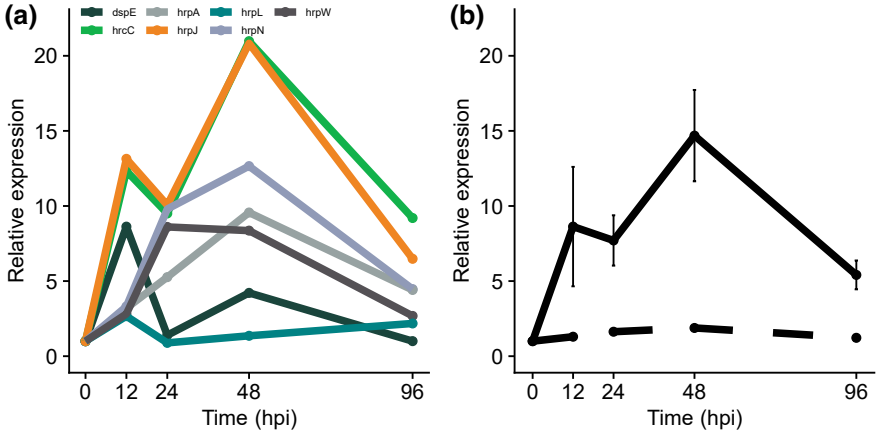

FIGURE 2 Temporal expression patterns of flagellar and type III secretion system (T3SS) genes during flower infection, relative to inoculum. (a) Average expression patterns for each T3SS cluster operon, labelled by the first gene in the operon. (b) Average expression pattern across all T3SS genes, solid line with error bars showing standard error, and *hrpL* expression pattern, dashed line. (c) Average expression pattern of each of the six flagellar gene clusters in the ATCC 49946 chromosome. (d) Average expression pattern of all flagellar genes with error bars showing standard error

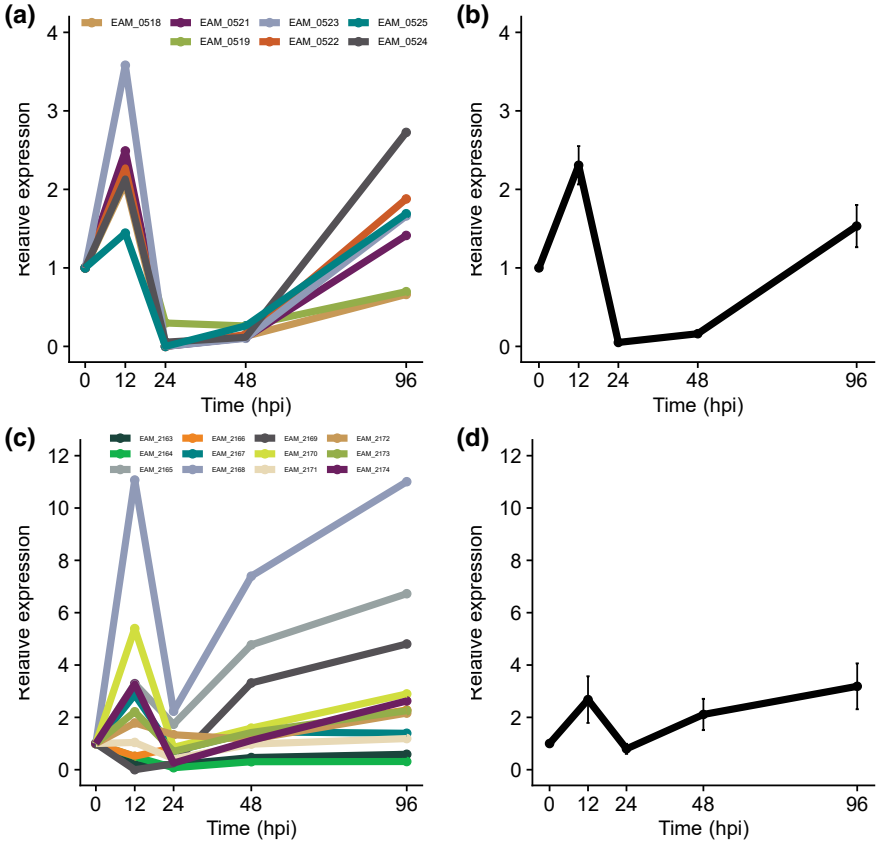

FIGURE 3 Temporal expression patterns of select sugar-related genes during flower infection, relative to inoculum. (a) Expression pattern for all sorbitol utilization genes. (b) Average expression pattern for all sorbitol utilization genes. (c) Expression pattern of all amylovoran biosynthesis genes. (d) Average expression patterns of amylovoran biosynthesis genes. Error bars represent standard error

2.4 | Exopolysaccharide and sugar utilization gene expression profiles

To succeed in building populations that will facilitate infection and overcome host defences, *E. amylovora* must efficiently utilize the available carbon sources. In apple tissues, the primary storage and transport sugar is sorbitol (Raese et al., 1977). In our expression data, we found that sorbitol utilization genes were induced on the flower stigma, then shut off when the cells were in the nectary area, and then expressed again in flower pedicels (Figure 3a,b). The down-regulation of sorbitol utilization genes in the flower base and nectary of the flower corresponds to an abundance of sucrose, but not sorbitol, in nectar (Tóth et al., 2003).

Production of the exopolysaccharide amylovoran is essential for *E. amylovora* pathogenicity (Bernhard et al., 1993). In our expression data, we found that the amylovoran biosynthetic genes were induced on the stigma, shut off early in the flower base and then induced again after 48 h in the flower base and also in the pedicel (Figure 3c,d). This expression pattern is similar to that of the sorbitol utilization genes, and linear regression showed a positive correlation between expression profiles of sorbitol utilization and amylovoran biosynthesis genes ($R^2 = 0.426$; Figure S4a). To show that these correlations are specific, we observed no correlation between expression of amylovoran biosynthesis genes and T3SS genes ($R^2 = 0.066$; Figure S4b). Interestingly, genes involved in the regulation and biosynthesis of the exopolysaccharide levan, a homopolymer of fructose synthesized from sucrose, showed increased expression at 24 hpi in the flower base at the time when both amylovoran and sorbitol genes were down-regulated (data not shown). Furthermore, genes involved in metabolism of sucrose were not up-regulated in the flower base (data not shown), where sucrose would be abundant, suggesting that during infection of the flower base and nectary, *E. amylovora* is primarily converting sucrose to levan, but is not largely using the sucrose as a carbon source, consistent with the observation that under osmotic stress in nectar *E. amylovora* cells do not typically divide (Ivanoff & Keitt, 1941).

2.5 | High expression under infection co-expressors

We hypothesized that genes with expression that increased on apple flower infection, and where that increased expression was maintained across time points and tissues, were likely to represent genes that are important for *E. amylovora* during disease. Such genes are likely to be essential for successful infection by virtue of function as virulence factors and not simply due to major growth defects. To identify genes that match these criteria, we generated a numerical vector representing this expression pattern of interest and searched across all genes for genes with a statistically significant ($p < 0.05$) Pearson's correlation to the sample vector. We identified 16 genes with significant similarity to the target expression pattern, and corresponding expression profiles are represented in Figure 4. The identities of these genes and the putative functions of their products are specified in Table 1. Among these genes with induced and maintained expression we found *waaL*, an O-antigen ligase gene that has previously been demonstrated to be a virulence factor for *E. amylovora* (Berry et al., 2009). Interestingly, a significant number of these genes (*iscS*, *tpx*, *cysG*, *masA*, and *dsbA*) are all involved in sulphur metabolism or maintenance of sulphur

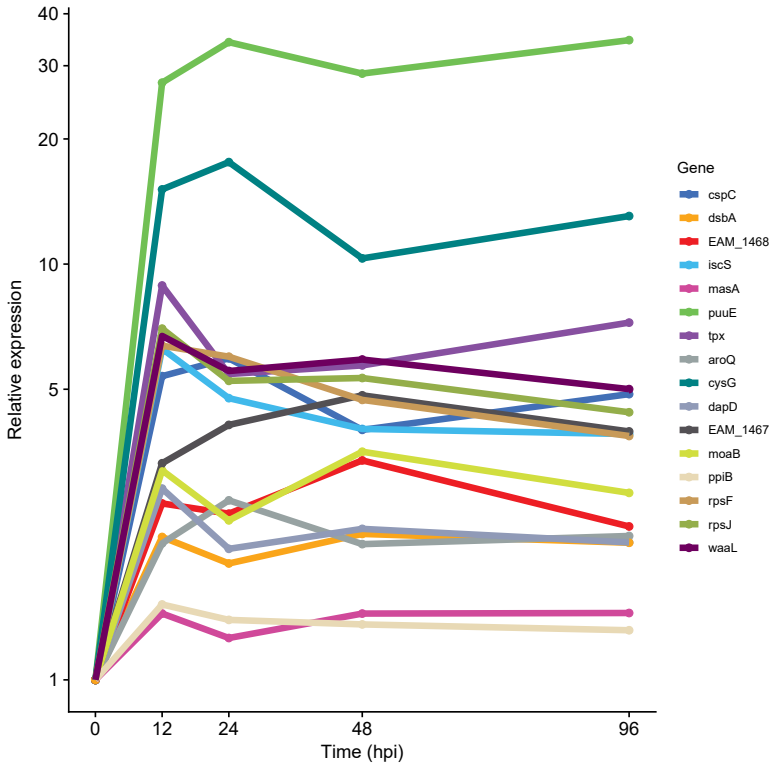

FIGURE 4 Expression pattern of 16 identified genes in which expression is induced and sustained during flower infection across time and tissues

TABLE 1 *Erwinia amylovora* genes with expression induced and maintained on apple flowers under field conditions

Gene name	Locus TAG	Putative function	Fold induction[a]
puuE	EAM_2305	Putrescine utilization	31.2
cysG	EAM_2691	Cysteine biosynthesis	14.0
tpx	EAM_1833	Thiol-peroxidase	6.8
waaL	EAM_0086	O-antigen ligase	5.8
rpsJ	EAM_3199	Ribosome small subunit protein	5.5
rpsF	EAM_0448	Ribosome small subunit protein	5.2
cspC	EAM_1967	Cold shock protein	5.0
iscS	EAM_2492	Iron-sulphur cluster formation and repair	4.7
–	EAM_1467	Putative nucleotide-binding protein	4.1
moaB	EAM_1219	Molybdenum cofactor	3.0
–	EAM_1468	Putative lipoprotein	2.7
dapD	EAM_0816	Lysine biosynthesis	2.3
aroQ	EAM_3140	Shikimate biosynthesis	2.3
dsbA	EAM_0025	Disulphide bond formation	2.1
masA	EAM_0886	Methionine salvage pathway	1.4
ppiB	EAM_1062	Proline isomerization, protein folding	1.4

[a]Average fold induction across all tissues and time points.

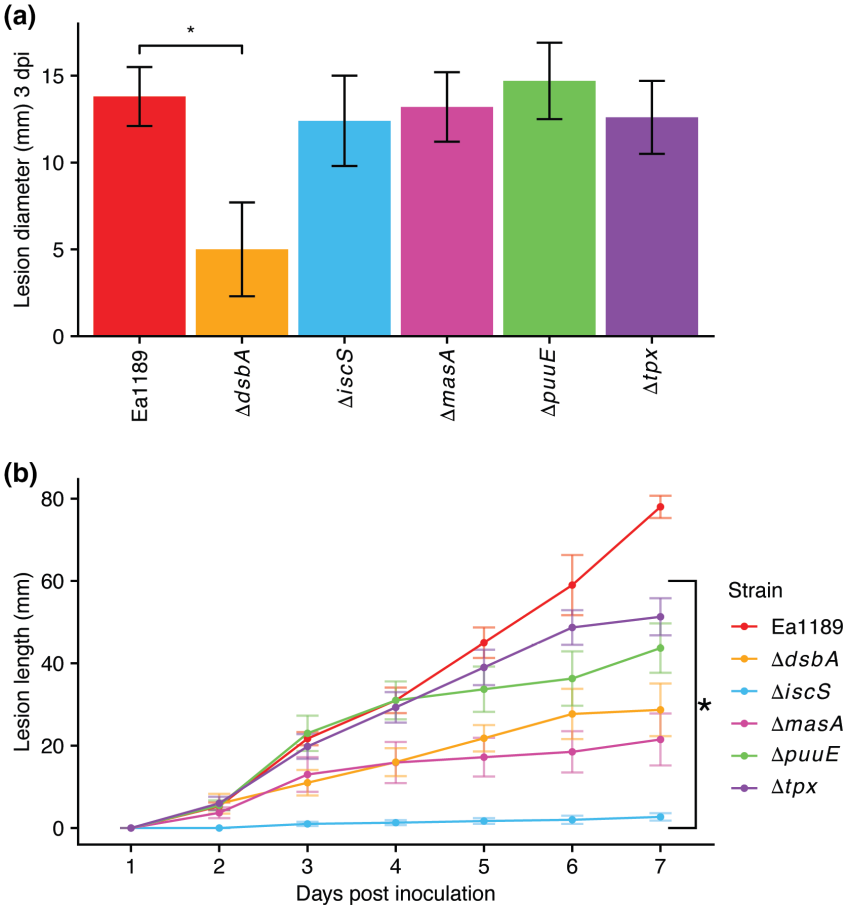

FIGURE 5 Virulence of indicated deletion mutant strains when inoculated onto (a) immature pears or (b) apple shoots. Asterisks indicate significant difference ($p < 0.05$) from wild-type *Erwinia amylovora* Ea1189 by Student's *t* test

oxidation status ($p < 0.0001$ by Fisher's exact test). We selected five of the 16 genes (*iscS*, *tpx*, *masA*, *puuE*, and *dsbA*) to generate knockout mutants and characterize their impacts on virulence and virulence-associated traits.

2.6 | Growth and virulence of knockout mutants

We hypothesized that genes with low expression in *E. amylovora* cells grown in LB medium but highly expressed during flower infection may be important for virulence, but dispensable to growth. Therefore, we tested the deletion mutant strains for effects on growth and virulence. When grown in LB medium, only the Δ*iscS* deletion mutant displayed slower growth than wild-type *E. amylovora* strain Ea1189 (Figure S5). The Δ*iscS* mutant had a longer lag phase and slower entry to exponential growth, but ultimately reached the same OD_{600} as the wild-type cells.

When inoculated onto immature pear fruits, the Δ*dsbA* mutant exhibited reduced development of disease symptoms at 3 dpi (Figure 5a). When inoculated onto apple shoots, all of the deletion mutants tested had reduced symptom development relative to wild-type *E. amylovora* strain Ea1189 at 7 dpi (Figure 5b). In apple shoots, the Δ*iscS* deletion mutant had nearly no symptom development, even 7 dpi. The remaining mutants displayed initial symptom progression similar to wild-type *E. amylovora* strain Ea1189, but later disease progression was delayed. The Δ*masA* and Δ*dsbA* mutants started to show reduced symptom development 4 dpi, and the Δ*puuE* and Δ*tpx* mutants did not manifest reduced symptom development until 6 and 7 dpi (Figure 5b). The virulence of all complemented mutant strains was restored to wild-type levels (Figure S9).

2.7 | Mutants and oxidative stress

Because all of the deletion mutants exhibited reduced symptom development when inoculated on apple shoots, and several of the deletion mutants are predicted to function in sulphur cycling or maintenance of sulphur oxidation state, we tested whether these mutants have altered catalase activity or altered susceptibility to exogenous hydrogen peroxide. We observed significantly reduced catalase activity in the Δ*puuE*, Δ*tpx*, and Δ*iscS* mutants, but only the Δ*tpx* and Δ*iscS* mutants were more susceptible to exogenous hydrogen peroxide than wild-type *E. amylovora* strain Ea1189 (Figure 6). Susceptibility to exogenous hydrogen peroxide was diminished, and catalase activity was partially restored in complemented strains (Figure S10).

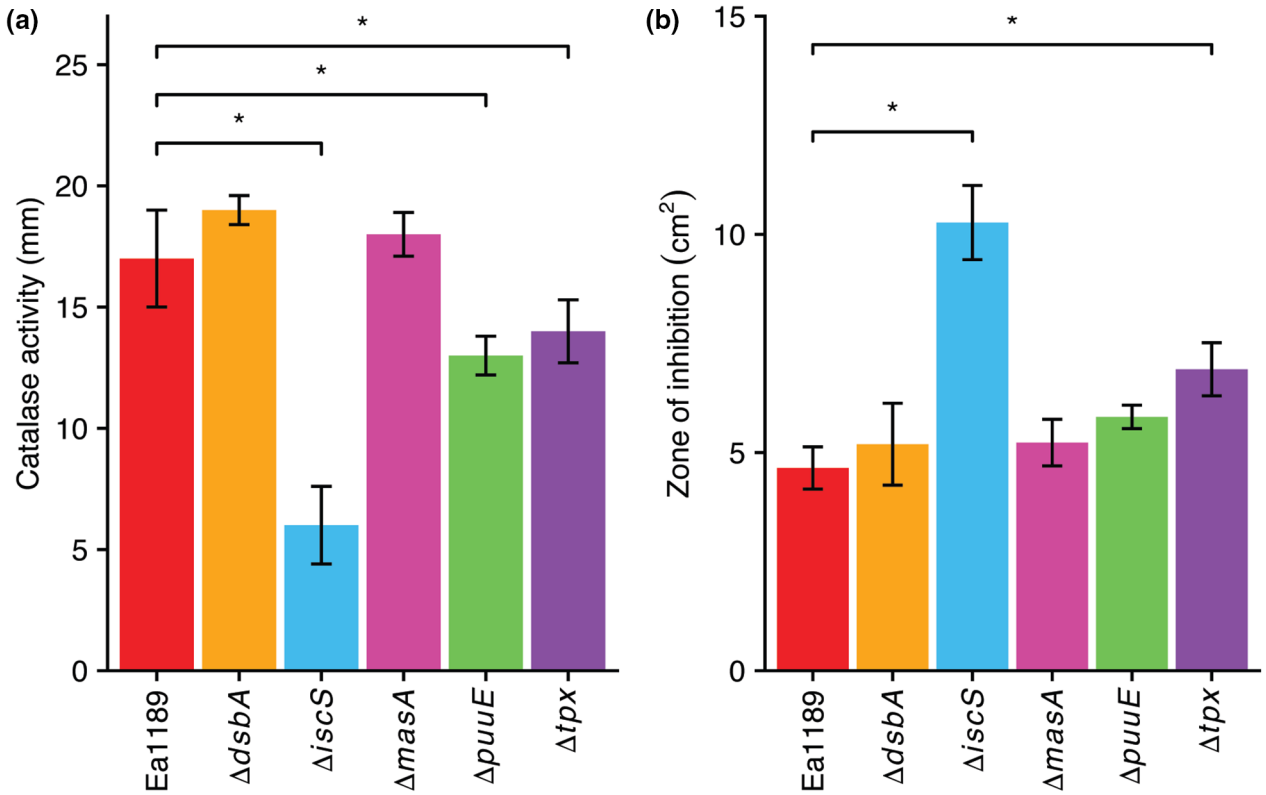

FIGURE 6 Deletion mutants have reduced catalase activity and Δ*iscS* has increased susceptibility to exogenous hydrogen peroxide. (a) Relative intracellular catalase activity of cells grown overnight in Luria-Bertani (LB) medium. (b) Zone of inhibition of indicated strains around a disk containing hydrogen peroxide on solid LB medium. Asterisks indicate significant ($p < 0.05$) difference compared to wild-type *Erwinia amylovora* Ea1189 by Student's *t* test

2.8 | Mutants and other virulence-associated traits

We further assessed the effects of mutations in these genes of interest by evaluating the mutant strains for a variety of virulence-associated traits. The Δ*masA* deletion mutant produced significantly more ($p < 0.05$) amylovoran and the Δ*iscS* and Δ*dsbA* deletion mutants produced significantly less amylovoran than wild-type *E. amylovora* strain Ea1189 (Figure 7a). The Δ*tpx* mutant exhibited significantly increased levansucrase activity, but the Δ*iscS* and Δ*puuE* mutants exhibited significantly reduced levansucrase activity relative to wild-type *E. amylovora* strain Ea1189 (Figure 7b). When assessed for biofilm formation, growth of the Δ*masA* and Δ*dsbA* mutants resulted in significantly greater crystal violet staining of adherent cells (Figure 7c). Only the Δ*dsbA* mutant had a significant reduction in swimming motility relative to wild-type *E. amylovora* strain Ea1189 (Figure 7d). Functions of virulence-associated traits returned to levels equivalent to Ea1189 in complemented mutant strains, except for Δ*puuE*+pBBR1MCS5 *puuE*::*puuE* (Figure S11).

3 | DISCUSSION

We report novel *E. amylovora* single-gene deletion mutants impacting virulence and virulence factors that were identified through a temporal transcriptomic analysis of *E. amylovora* gene expression during disease progression on apple flowers in the field. This analysis also agrees with previously reported T3SS gene expression patterns during flower infection, as well as hypotheses for the roles of virulence traits during early stages of infection, summarized in Figure 8.

Genes encoding the T3SS and flagellar systems were induced during early stages of infection on flower stigmas and in the flower base, but expression decreased during later infection stages in the pedicel. This expression pattern, along with the correlation between expression of flagellar genes and T3SS genes, supports the infection model in which *E. amylovora* must actively migrate down the flower stigma, swim through nectar, and then suppress host defences to invade the base of the flower through natural openings. Although the T3SS and flagella may continue to be expressed during later stages of infection, their highest expression occurred during early-stage infection, suggesting that they are of greatest importance during these infection stages.

RNA-Seq expression patterns indicate that amylovoran production and sorbitol utilization genes were initially expressed on the stigma, but then expression decreased in the flower base and increased again in flower pedicels. Because of the sucrose levels in the nectary, which can range from 10% to 50% (Tóth et al., 2003), we hypothesize that *E. amylovora* has little need for sorbitol utilization genes in this environment and this is the reason for decreased expression. A correlation between sorbitol utilization and amylovoran production was previously observed (Geider et al., 1996; Wang et al., 2010) and our data support this observation. We hypothesize that in nectar, where sucrose levels are high, the bacteria do not need to produce amylovoran because they are not interacting directly with host cells nor actively forming biofilms. Whether this correlation is due to co-regulation of sorbitol utilization and amylovoran production genes must still be determined.

Among genes with consistently increased expression in all tissues and time points sampled, we identified a group of novel virulence-associated genes, which includes several genes involved in sulphur cycling and maintenance of sulphur-oxidation status, possibly through helping *E. amylovora* to cope with oxidative stresses. These genes were induced by *E. amylovora* during flower infection and high expression was sustained across the tissues and time points sampled. Testing of these genes that were highly expressed throughout flower infection confirmed that deletion of these genes results in virulence defects.

We constructed single deletion mutants of five genes with consistently higher expression across tissues and time points during infection of apple flowers: Δ*dsbA*, Δ*iscS*, Δ*masA*, Δ*puuE*, and Δ*tpx*. Decreased symptom development was observed when each of these deletion mutants was inoculated on susceptible apple shoots, but only the Δ*dsbA* mutant showed virulence defects relative to wild-type *E. amylovora* Ea1189 when inoculated on immature pears.

Disulphide bond formation protein A (DsbA) enzymatically carries thiol disulphide oxidoreductase activity and plays an important role in the appropriate formation of disulphide bonds in other proteins in the periplasm (Akiyama et al., 1992; Wunderlich & Glockshuber, 1993). Several secreted proteins rely on DsbA for disulphide bond formation to facilitate proper secretion (Schierle et al., 2003). Deletion of *dsbA* resulted in reduced virulence on immature pears and on apple shoots. The Δ*dsbA* mutant was also affected in flagellar motility, a known effect of losing *dsbA* function in *Escherichia coli* (Dailey & Berg, 1993). In *E. amylovora*, deletion of *dsbA* resulted in low amylovoran production and high crystal violet staining in a biofilm assay, suggesting this mutant may affect attachment structures because deletion of the RNA chaperone *hfq* also results in reduced amylovoran production but high crystal violet staining in biofilm assays due to a hyperattachment phenotype (Zeng et al., 2013).

The iron-sulphur cluster synthesis protein IscS is a cysteine desulphurase and a critical enzyme in formation of iron-sulphur clusters for loading into many other cellular enzymes (Schwartz et al., 2000; Takahashi & Nakamura, 1999; Urbina et al., 2001). With its enzymatic function, IscS plays an important role in repair of oxidatively damaged iron-sulphur clusters, and *E. coli iscS* deletion mutants exhibit increased susceptibility to hydrogen peroxide (Rogers et al., 2003; Yang et al., 2002). We also observed increased susceptibility to hydrogen peroxide in the *E. amylovora* Δ*iscS* mutant as well as decreased catalase activity. IscS is also required for thiamin biosynthesis in *E. coli*, specifically involved in biosynthesis of the thiazole moiety of thiamin via sulphur transfer to the C-terminal carboxylate of ThiS, a small sulphur-carrier protein (Begley et al., 1999; Lauhon & Kambampati, 2000). We have previously shown that thiamin biosynthesis in *E. amylovora* stimulates the function of the tricarboxylic acid cycle, thereby providing energy requirements for amylovoran biosynthesis (Yuan et al., 2021). The Δ*iscS* mutant

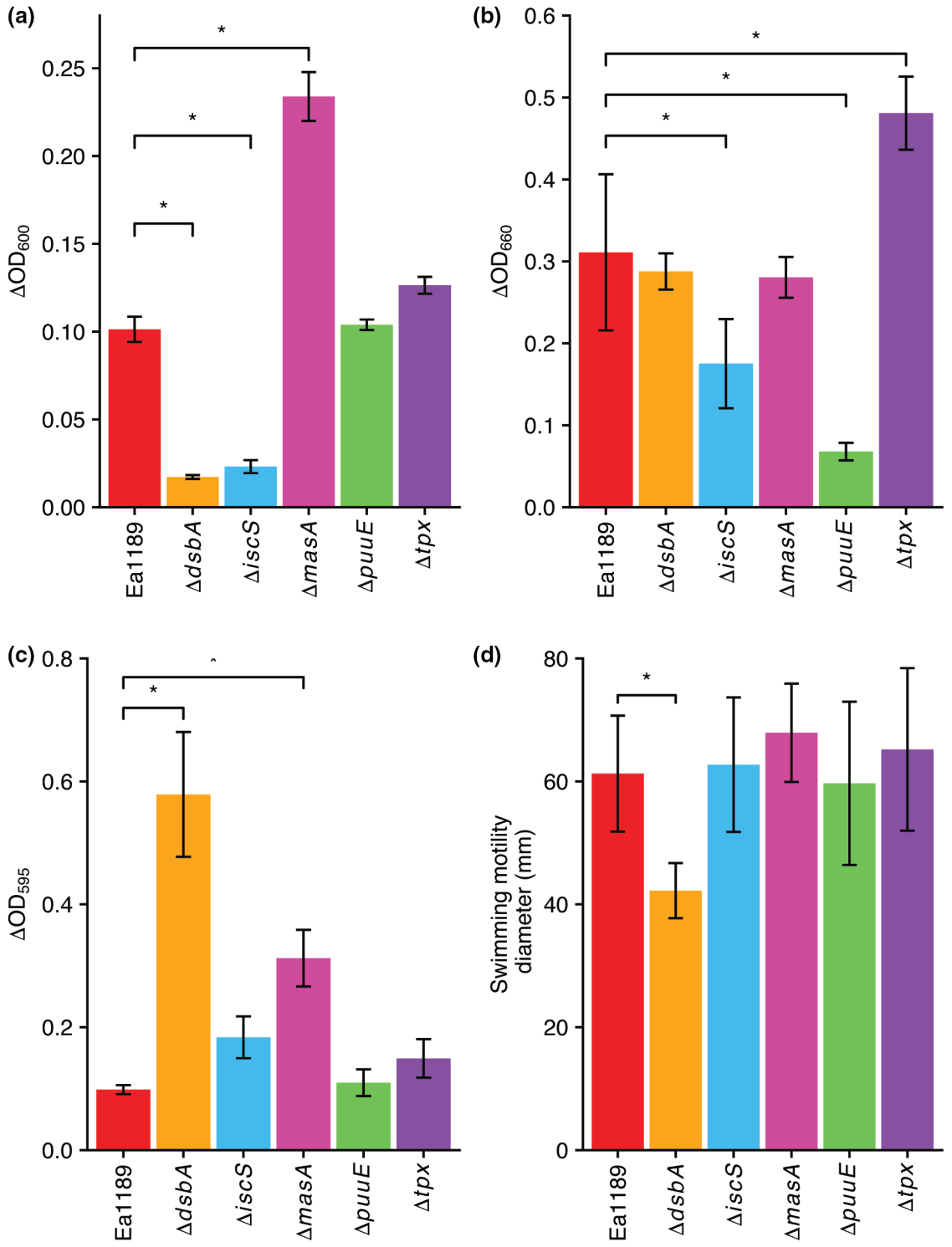

FIGURE 7 Deletion of genes affecting virulence also affects other virulence-associated traits. (a) Amylovoran production by cells grown in modified basal medium A (MBMA). (b) Levansucrase activity secreted into supernatants of cultures grown in Luria-Bertani medium. (c) Biofilm formation as assessed by crystal violet staining following 48 h of static growth in MBMA. (d) Swimming motility of indicated strains stab-inoculated into soft agar (0.25% wt/vol) and incubated for 24 h. Asterisks indicate significant ($p < 0.05$) difference from wild-type *E. amylovora* Ea1189 by Student's *t* test

exhibited decreased production of the exopolysaccharides amylovoran and levan, a slight growth defect in LB medium, and reduced catalase activity relative to wild-type cells. Although it did not display reduced symptom development when inoculated on immature pears, the Δ*iscS* mutant was avirulent on apple shoots. Recent work indicates that oxidative stress due to hydrogen peroxide affects *E. amylovora* survival (Santander et al., 2018). Given this result, we hypothesize that the loss of virulence in the Δ*iscS* mutant in apple

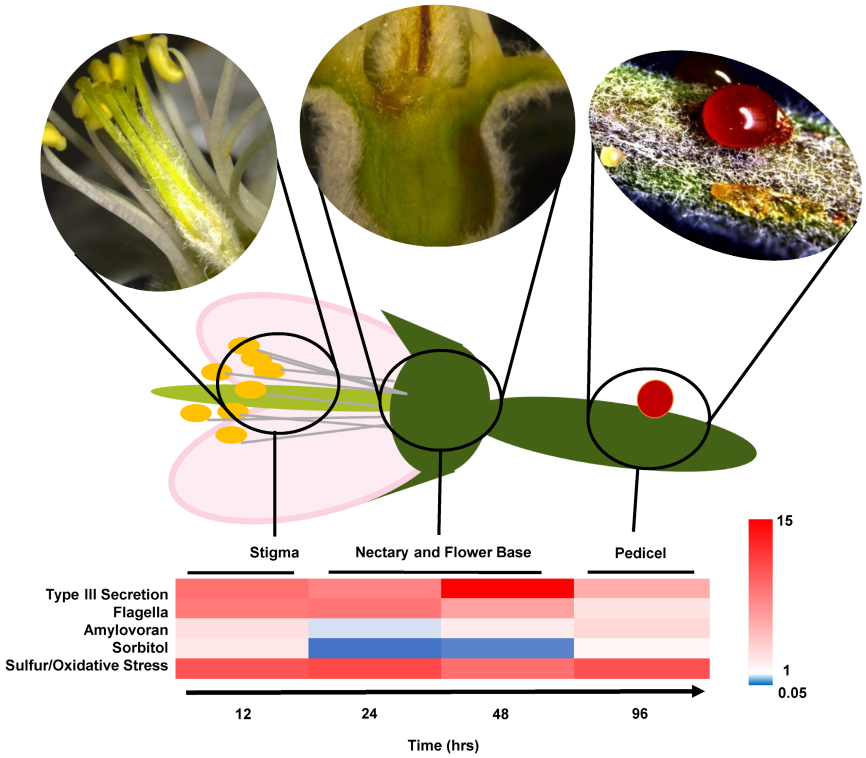

FIGURE 8 Representation of apple flower tissues and heat map of average expression across time of virulence-associated traits. The type III secretion and flagellar systems are strongly induced early during infection on flower stigmas and in the flower base, but expression decreases later during infection in the pedicel. Amylovoran production and sorbitol utilization genes are initially expressed on the stigma, but decreased in expression in the flower base and increased again in flower pedicels. We identified a group of novel virulence genes, which includes several genes involved in sulphur cycling and maintenance of sulphur-oxidation status, probably through helping *Erwinia amylovora* to cope with oxidative stresses. These genes are induced by *E. amylovora* during flower infection and high expression is sustained across the tissues and time points sampled

shoots is due to inability to cope with oxidative stress from host defences.

As determined for DsbA and IscS, thiol peroxidase Tpx is involved in cycling of the sulphur oxidative state (Baker & Poole, 2003; Kim et al., 1999). The *E. amylovora tpx* deletion mutant did not have a virulence defect in immature pears, but it was reduced in virulence in apple shoots. Deletion of *tpx* also had a small but significant effect on catalase activity and susceptibility to hydrogen peroxide. This is consistent with Tpx roles reported in *Salmonella typhimurium*, where deletion of *tpx* increases susceptibility to hydrogen peroxide and decreases bacterial survival in macrophages (Horst et al., 2010).

In addition to DsbA, IscS, and Tpx, which have direct roles in sulphur redox chemistry, MasA participates in sulphur recycling through the methionine salvage pathway (Albers, 2009). Sulphur utilization and sulphur stress are linked to ability to cope with oxidative stresses. We hypothesize that these genes that are up-regulated during host infection and are involved in sulphur cycling play critical roles during disease development by enabling *E. amylovora* to cope with host-derived reactive oxygen species. This hypothesis is supported by the observed decreases in virulence as well as the increased susceptibility to hydrogen peroxide in the Δ*tpx* and Δ*iscS* deletion mutants.

The Δ*puuE* deletion mutant does not have direct links to sulphur metabolism, and it is possible that the PuuE protein is playing another important role in disease progression on apple flowers and shoots. It was recently demonstrated that putrescine utilization is important for disease progression in *Ralstonia solanacearum* during xylem colonization in tomatoes (Lowe-Power et al., 2018). It is possible that putrescine uptake and utilization in *E. amylovora* is similarly important during infection because both *E. amylovora* and *R. solanacearum* colonize host xylem.

In summary, we identified five new deletion mutants with reduced virulence on apple shoots in this work through gene expression pattern analysis of *E. amylovora* RNA-Seq data during apple flower infection under field conditions. We specifically identified genes based on an expression pattern in which RNA abundance was low in cells grown in LB medium and used for plant inoculations, but high and sustained across apple flower tissues and time points. Future efforts to characterize the specific functions that affect the virulence of the proteins encoded by these genes will provide greater understanding of the roles they play that are important during infection but dispensable during growth in rich medium. Because we only identified novel factors based on a single expression pattern, our gene expression data set can be further used to identify additional novel genes and traits that are important during specific stages of fire blight disease progression.

4 | EXPERIMENTAL PROCEDURES

4.1 | Culture conditions, growth, and plasmids

E. amylovora strains were grown routinely using LB medium at 28°C. For field inoculations, the Michigan strain *E. amylovora* Ea110 (Zhao et al., 2005) was used. For generation of genetic mutants and virulence trait analysis, *E. amylovora* strain Ea1189 (McNally et al., 2012) was used. Gene deletion mutants were generated using a Red-recombinase approach as described (Datsenko & Wanner, 2000). Bacterial strains and oligonucleotides used in this work are included in Tables 2 and S2, respectively. Deletion mutants were complemented by constructing plasmids from the pBBR1MCS-5 plasmid with gentamicin resistance backbone and gBlocks (IDT-DNA) containing the gene of interest and the native promoter.

4.2 | Field inoculations, cultivar, and sampling

Apple flowers of the cultivar McIntosh were inoculated with a 1-μl droplet of *E. amylovora* Ea110 that was previously grown overnight in liquid LB medium. All flowers were inoculated on the day immediately following flower opening. For RNA-Seq samples, inoculations occurred on 6 May 2019 at 11:00 (0 hpi). Weather conditions corresponding to the time course of the experiment can be found in Table S2. Four biological replicates were collected for each tissue × time point combination and some samples were later discarded due to low RNA quality. For stigmas, each biological replicate consisted of inoculated stigmas pooled from 15 to 20 flowers. For flower base, each biological replicate was a pool from four inoculated flowers. Biological replicates of pedicel samples were pooled from two pedicels. Stigma inoculations were conducted using a cell density of 10^9 cfu/ml (10^6 cfu inoculated per flower) and stigma samples were collected 12 hpi. For all other samples, the flower nectary was inoculated with a 1-μl droplet with cell density of 10^8 cfu/ml (10^5 cfu/flower). Of these samples, the base of the flower was sampled at 24 and 48 hpi. For these samples the base was considered to be the remaining portion of the flower following removal of petals, anthers, stigmas, and pedicels. Inoculated flowers were monitored for emergence of ooze droplets from flower pedicels. When ooze appeared, the ooze droplet was removed and the pedicel was sampled. This occurred at approximately 96 hpi.

TABLE 2 Bacterial strains used in this work and their relevant characteristics

Bacterial strains	Relevant characteristics	Source or reference
Erwinia amylovora		
Ea110	Michigan-native wild-type	Ritchie and Klos (1976)
Ea1189	Wild-type strain for genetic studies	GSPB[a]
Ea1189 Δ*dsbA*	*dsbA* deletion mutant	This work
Ea1189 Δ*iscS*	*iscS* deletion mutant	This work
Ea1189 Δ*masA*	*masA* deletion mutant	This work
Ea1189 Δ*puuE*	*puuE* deletion mutant	This work
Ea1189 Δ*tpx*	*tpx* deletion mutant	This work
Ea1189 Δ*dsbA* + pBBR1MCS5 *dsbA*::*dsbA*	*dsbA* complemented mutant, native promoter	This work
Ea1189 Δ*iscS* + pBBR1MCS5 *iscS*::*iscS*	*iscS* complemented mutant, native promoter	This work
Ea1189 Δ*masA* + pBBR1MCS5 *masA*::*masA*	*masA* complemented mutant, native promoter	This work
Ea1189 Δ*puuE* + pBBR1MCS5 *puuE*::*puuE*	*puuE* complemented mutant, native promoter	This work
Ea1189 Δ*tpx* + pBBR1MCS5 *tpx*::*tpx*	*tpx* complemented mutant, native promoter	This work
Ea1189 + pBBR1MCS5	Control, empty vector Gm^R	Castiblanco(unpublished)
Escherichia coli		
DH5α	F^-80d*lacZ*1M151(*lacZYA-argF*) U169 *endA1 recA1 hsdR17* ($r_k^-m_k^+$)*deoR thi-1 supE44 gyrA96 relA1*λ^-	Invitrogen
Plasmids		
pBBR1MCS5	Broad-host-range cloning vector, Gm^R	Kovach et al. (1995)

[a]GSPB, Göttinger Sammlung phytopathogener Bakterien, Göttingen, Germany.

4.3 | RNA extractions, library preparation, and sequencing

Total RNA was isolated from infected plant samples using the EZNA Plant kit (Omega) according to the manufacturer's recommendations, including the on-column DNase treatment, which was carried out using Turbo DNase I (Invitrogen). RNA was checked for quality and quantity using Caliper LabChip GX (Perkin Elmer) and Qubit RNA HS (Thermo Fisher Scientific) analysis, respectively. To enrich RNA samples for bacterial messenger RNA, multiple depletion reagents were used, including oligo(dT) beads to deplete eukaryotic polyadenylated mRNA, RiboZero Plant rRNA removal beads to deplete host rRNA, and RiboZero bacterial rRNA removal beads to remove prokaryotic rRNA (Illumina). The remaining RNA was used for library preparation using an Illumina TruSeq Stranded Total RNA Library Preparation Kit (Illumina) on a Sciclone G3 robot following the manufacturer's recommendations (Perkin Elmer). Library quality was assessed using Caliper LabChipGX HS DNA (Perkin Elmer) and Qubit dsDNA HS (Thermo Fisher Scientific) assays. Samples were pooled and run on three lanes using the Illumina HiSeq4000 platform with single-end 50 bp format. Sequencing was conducted at the Michigan State University Research Technology Support Facility. Base calling was conducted by Illumina Real Time Analysis v. 2.7.6.

4.4 | Sequence and computational analysis

RNA sequencing reads were trimmed using Trimmomatic (Bolger et al., 2014) and mapped to the *E. amylovora* ATCC 49946 genome (Sebaihia et al., 2010) using bowtie2 (Langmead & Salzberg, 2012). Mapped reads were counted in each annotated gene using HTseq (Anders et al., 2015). Read counts per gene by sample were normalized to total sample read counts, using total reads mapping to the *E. amylovora* genome as a proxy for bacterial population. Normalized read counts were statistically analysed for differential gene expression using the R package DESeq (Anders & Huber, 2012). For gene expression pattern analysis, Pearson's correlation coefficients and associated test statistics were calculated using R and the vector used to identify consistently up-regulated genes of interest was [1,10,10,10,10]. Principal component analysis, clustering analyses, and heat map generation were conducted using ClustVis (Metsalu & Vilo, 2015). RNA-Seq results were confirmed using RT-qPCR of 10 genes (Table S2) following the methods of Slack et al. (2017).

4.5 | Virulence assays

Immature pears were inoculated as described previously (Zhao et al., 2005). Immature pears were wounded and inoculated with 10^3 cfu in a 1-μl droplet and incubated in high-humidity chambers at 28°C. Necrotic or water-soaked lesion diameters were measured 4 dpi. Pear experiments were repeated three times with a total of at least 15 replicates per strain. Actively growing shoots of 2-year-old potted apple trees cultivar Gala were inoculated as described (Koczan et al., 2009). Briefly, shoots were cut with sterile scissors dipped in a bacterial suspension of 10^8 cfu/ml. Necrotic symptom development was monitored every 24 h and the distance from inoculation to the end of visible symptoms was measured at the indicated time points. Each replicate of a strain was inoculated onto a different tree. The shoot assay was repeated twice with at least six shoots per strain per experiment.

4.6 | Oxidative stress testing

Catalase activity was measured as described (Iwase et al., 2013). Susceptibility to exogenous hydrogen peroxide was assessed through a described zone of inhibition approach (Santander et al., 2018). Briefly, overnight cell cultures were adjusted to an OD_{600} of 0.2 and 100 μl of cells were plated onto solid LB medium. A filter paper disc was placed on each plate and treated with 10 μl of 8 M H_2O_2. Following 24 h of growth at 28°C, plates were imaged and the zone of inhibition around each disc was measured using ImageJ (Abràmoff et al., 2004). Each phenotype was tested four times with at least three replicates per strain.

4.7 | Virulence-associated trait analysis

Virulence-associated traits were assessed using established methods. Virulence phenotypes were tested three times independently for a total of at least 12 replicates per strain. Production of the exopolysaccharide amylovoran was assessed following growth for 48 h in modified basal medium A (MBMA; 3 g/L KH_2PO_4, 7 g/L K_2HPO_4, 1 g/L $(NH_4)_2SO_4$, 2 ml/L glycerol, 0.5 g/L citric acid, 0.03 g/L $MgSO_4$, 10 g/L sorbitol) at 28°C as described (Bellemann et al., 1994; Edmunds et al., 2013; Zhao et al., 2009). To quantify levansucrase activity, culture supernatants were mixed in a 1:1 ratio with 2 M sucrose, incubated for 24 h, and the resulting turbidity was measured as described (Geier & Geider, 1993). Biofilm formation for each strain was determined using 96-well microtitre plates as described (Santander & Biosca, 2017). Swimming motility was assessed following stab inoculation of cells into soft-agar plates (0.25% wt/vol) using a described method (Zeng & Sundin, 2014).

ACKNOWLEDGEMENTS

This project was supported by the Agriculture and Food Research Initiative competitive grant no. 2015-67013-23068 of the US Department of Agriculture National Institute of Food and Agriculture, Michigan State University AgBioResearch, and Project GREEEN, a Michigan plant agriculture initiative at Michigan State University. This material is also based on work supported by the National Science Foundation Graduate Research Fellowship under grant no. DGE1424871 to J.K.S.

CONFLICT OF INTEREST

The authors declare that they have no conflicts of interest.

AUTHOR CONTRIBUTIONS

J.K.S. and G.W.S. conceived of and designed the experiments. J.K.S., K.G., and I.P. conducted the experiments. J.K.S., K.G., I.P., and G.W.S. analysed the data, and wrote and edited the manuscript.

DATA AVAILABILITY STATEMENT

The sequencing datasets generated in this study can be found in the NCBI sequence read archive (SRA) at https://www.ncbi.nlm.nih.gov/bioproject/587128 under BioProject accession number PRJNA587128.

ORCID

Jeffrey K. Schachterle https://orcid.org/0000-0002-6506-2398
Kristi Gdanetz https://orcid.org/0000-0002-8916-7602
George W. Sundin https://orcid.org/0000-0003-4078-8368

REFERENCES

Abràmoff, M.D., Magalhães, P.J. & Ram, S.J. (2004) Image processing with ImageJ. *Biophotonics International*, 11, 36–42.

Akiyama, Y., Kamitani, S., Kusukawa, N. & Ito, K. (1992) In vitro catalysis of oxidative folding of disulfide-bonded proteins by the *Escherichia coli dsbA* (*ppfA*) gene product. *Journal of Biological Chemistry*, 267, 22440–22445.

Albers, E. (2009) Metabolic characteristics and importance of the universal methionine salvage pathway recycling methionine from 5′-methylthioadenosine. *IUBMB Life*, 61, 1132–1142.

Ancona, V., Lee, J.H. & Zhao, Y. (2016) The RNA-binding protein CsrA plays a central role in positively regulating virulence factors in *Erwinia amylovora*. *Scientific Reports*, 6, 37195.

Anders, S. & Huber, W. (2012) *Differential expression of RNA-Seq data at the gene level–the DESeq package*. Heidelberg, Germany: European Molecular Biology Laboratory (EMBL).

Anders, S., Pyl, P.T. & Huber, W. (2015) HTSeq—a Python framework to work with high-throughput sequencing data. *Bioinformatics*, 31, 166–169.

Baker, C.J., Orlandi, E.W. & Mock, N.M. (1993) Harpin, an elicitor of the hypersensitive response in tobacco caused by *Erwinia amylovora*, elicits active oxygen production in suspension cells. *Plant Physiology*, 102, 1341–1344.

Baker, L.M. & Poole, L.B. (2003) Catalytic mechanism of thiol peroxidase from *Escherichia coli*. Sulfenic acid formation and overoxidation of essential CYS61. *Journal of Biological Chemistry*, 278, 9203–9211.

Barny, M.-A. (1995) *Erwinia amylovora hrpN* mutants, blocked in harpin synthesis, express a reduced virulence on host plants and elicit variable hypersensitive reactions on tobacco. *European Journal of Plant Pathology*, 101, 333–340.

Bayot, R.G. & Ries, S.M. (1986) Role of motility in apple blossom infection by *Erwinia amylovora* and studies of fire blight control with attractant and repellent compounds. *Phytopathology*, 76, 441–445.

Begley, T.P., Xi, J., Kinsland, C., Taylor, S. & Mclafferty, F. (1999) The enzymology of sulfur activation during thiamin and biotin biosynthesis. *Current Opinion in Chemical Biology*, 3, 623–629.

Bellemann, P., Bereswill, S., Berger, S. & Geider, K. (1994) Visualization of capsule formation by *Erwinia amylovora* and assays to determine amylovoran synthesis. *International Journal of Biological Macromolecules*, 16, 290–296.

Bernhard, F., Coplin, D.L. & Geider, K. (1993) A gene cluster for amylovoran synthesis in *Erwinia amylovora*: characterization and relationship to *cps* genes in *Erwinia stewartii*. *Molecular and General Genetics*, 239, 158–168.

Berry, M.C., McGhee, G.C., Zhao, Y. & Sundin, G.W. (2009) Effect of a *waaL* mutation on lipopolysaccharide composition, oxidative stress survival, and virulence in *Erwinia amylovora*. *FEMS Microbiology Letters*, 291, 80–87.

Bogdanove, A.J., Bauer, D.W. & Beer, S.V. (1998) *Erwinia amylovora* secretes DspE, a pathogenicity factor and functional AvrE homolog, through the Hrp (type III secretion) pathway. *Journal of Bacteriology*, 180, 2244–2247.

Bolger, A.M., Lohse, M. & Usadel, B. (2014) Trimmomatic: a flexible trimmer for Illumina sequence data. *Bioinformatics*, 30, 2114–2120.

Castiblanco, L.F. & Sundin, G.W. (2018) Cellulose production, activated by cyclic di-GMP through BcsA and BcsZ, is a virulence factor and an essential determinant of the three-dimensional architectures of biofilms formed by *Erwinia amylovora* Ea1189. *Molecular Plant Pathology*, 19, 90–103.

Dailey, F.E. & Berg, H.C. (1993) Mutants in disulfide bond formation that disrupt flagellar assembly in *Escherichia coli*. *Proceedings of the National Academy of Sciences of the United States of America*, 90, 1043–1047.

Datsenko, K.A. & Wanner, B.L. (2000) One-step inactivation of chromosomal genes in *Escherichia coli* K-12 using PCR products. *Proceedings of the National Academy of Sciences of the United States of America*, 97, 6640–6645.

Dellagi, A., Brisset, M.-N., Paulin, J.-P. & Expert, D. (1998) Dual role of desferrioxamine in *Erwinia amylovora* pathogenicity. *Molecular Plant-Microbe Interactions*, 11, 734–742.

Edmunds, A.C., Castiblanco, L.F., Sundin, G.W. & Waters, C.M. (2013) Cyclic di-GMP modulates the disease progression of *Erwinia amylovora*. *Journal of Bacteriology*, 195, 2155–2165.

Geider, K. (2000) Exopolysaccharides of *Erwinia amylovora*: structure, biosynthesis, regulation, role in pathogenicity of amylovoran and levan. In: Vanneste, J.L. (Ed.) *Fire blight: the disease and its causative agent, Erwinia amylovora*. Wallingford: CABI, pp. 117–140.

Geider, K., Aldridge, P., Bereswill, S., Bugert, P. & Langlotz, C. (1996) Characterization of exopolysaccharide synthesis by *Erwinia amylovora*. *Acta Horticulturae*, 411, 259–264.

Geier, G. & Geider, K. (1993) Characterization and influence on virulence of the levansucrase gene from the fireblight pathogen *Erwinia amylovora*. *Physiological and Molecular Plant Pathology*, 42, 387–404.

Gross, M., Geier, G., Rudolph, K. & Geider, K. (1992) Levan and levansucrase synthesized by the fireblight pathogen *Erwinia amylovora*. *Physiological and Molecular Plant Pathology*, 40, 371–381.

Horst, S.A., Jaeger, T., Denkel, L.A., Rouf, S.F., Rhen, M. & Bange, F.-C. (2010) Thiol peroxidase protects *Salmonella enterica* from hydrogen peroxide stress in vitro and facilitates intracellular growth. *Journal of Bacteriology*, 192, 2929–2932.

Ivanoff, S. & Keitt, G. (1941) Relations of nectar concentration to growth of *Erwinia amylovora* and fire blight infection of apple and pear blossoms. *Journal of Agricultural Research*, 62, 733–743.

Iwase, T., Tajima, A., Sugimoto, S., Okuda, K.-I., Hironaka, I., Kamata, Y. et al. (2013) A simple assay for measuring catalase activity: a visual approach. *Scientific Reports*, 3, 3081.

Kharadi, R.R., Schachterle, J.K., Yuan, X., Castiblanco, L.F., Peng, J., Slack, S.M. et al. (2021) Genetic dissection of the *Erwinia amylovora* disease cycle. *Annual Review of Phytopathology*, 59, 191–212.

Kim, S.J., Han, Y.H., Kim, I.H. & Kim, H.K. (1999) Involvement of ArcA and Fnr in expression of *Escherichia coli* thiol peroxidase gene. *IUBMB Life*, 48, 215–218.

Koczan, J.M., Lenneman, B.R., McGrath, M.J. & Sundin, G.W. (2011) Cell surface attachment structures contribute to biofilm formation and

xylem colonization of *Erwinia amylovora*. *Applied and Environmental Microbiology*, 77, 7031–7039.

Koczan, J.M., McGrath, M.J., Zhao, Y. & Sundin, G.W. (2009) Contribution of *Erwinia amylovora* exopolysaccharides amylovoran and levan to biofilm formation: implications in pathogenicity. *Phytopathology*, 99, 1237–1244.

Kovach, M.E., Elzer, P.H., Steven, Hill D., Robertson, G.T., Farris, M.A., Roop, R.M. & Peterson, K.M. (1995) Four new derivatives of the broad-host-range cloning vector pBBR1MCS, carrying different antibiotic-resistance cassettes. *Gene*, 166, 175–176.

Langmead, B. & Salzberg, S.L. (2012) Fast gapped-read alignment with Bowtie 2. *Nature Methods*, 9, 357.

Lauhon, C.T. & Kambampati, R. (2000) The *iscS* gene in *Escherichia coli* is required for the biosynthesis of 4-thiouridine, thiamin, and NAD. *Journal of Biological Chemistry*, 275, 20096–20103.

Li, W., Ancona, V. & Zhao, Y. (2014) Co-regulation of polysaccharide production, motility, and expression of type III secretion genes by EnvZ/OmpR and GrrS/GrrA systems in *Erwinia amylovora*. *Molecular Genetics and Genomics*, 289, 63–75.

Lowe-Power, T.M., Hendrich, C.G., Von Roepenack-Lahaye, E., Li, B., Wu, D., Mitra, R. et al. (2018) Metabolomics of tomato xylem sap during bacterial wilt reveals *Ralstonia solanacearum* produces abundant putrescine, a metabolite that accelerates wilt disease. *Environmental Microbiology*, 20, 1330–1349.

Malnoy, M., Martens, S., Norelli, J.L., Barny, M.-A., Sundin, G.W., Smits, T.H. et al. (2012) Fire blight: applied genomic insights of the pathogen and host. *Annual Review of Phytopathology*, 50, 475–494.

McNally, R.R., Toth, I.K., Cock, P.J., Pritchard, L., Hedley, P.E., Morris, J.A. et al. (2012) Genetic characterization of the HrpL regulon of the fire blight pathogen *Erwinia amylovora* reveals novel virulence factors. *Molecular Plant Pathology*, 13, 160–173.

Metsalu, T. & Vilo, J. (2015) ClustVis: a web tool for visualizing clustering of multivariate data using Principal Component Analysis and heatmap. *Nucleic Acids Research*, 43, W566–W570.

Nimtz, M., Mort, A., Domke, T., Wray, V., Zhang, Y., Qiu, F. et al. (1996) Structure of amylovoran, the capsular exopolysaccharide from the fire blight pathogen *Erwinia amylovora*. *Carbohydrate Research*, 287, 59–76.

Pester, D., Milčevičová, R., Schaffer, J., Wilhelm, E. & Blümel, S. (2012) *Erwinia amylovora* expresses fast and simultaneously *hrp/dsp* virulence genes during flower infection on apple trees. *PLoS One*, 7, e32583.

Piqué, N., Miñana-Galbis, D., Merino, S. & Tomás, J. (2015) Virulence factors of *Erwinia amylovora*: a review. *International Journal of Molecular Sciences*, 16, 12836–12854.

Puławska, J., Kałużna, M., Warabieda, W. & Mikiciński, A. (2017) Comparative transcriptome analysis of a lowly virulent strain of *Erwinia amylovora* in shoots of two apple cultivars – susceptible and resistant to fire blight. *BMC Genomics*, 18, 868.

Pusey, P. (2000) The role of water in epiphytic colonization and infection of pomaceous flowers by *Erwinia amylovora*. *Phytopathology*, 90, 1352–1357.

Raese, J., Williams, M. & Billingsley, H. (1977) Sorbitol and other carbohydrates in dormant apple shoots as influenced by controlled temperatures. *Cryobiology*, 14, 373–378.

Ramos, L.S., Lehman, B.L., Peter, K.A. & McNellis, T.W. (2014) Mutation of the *Erwinia amylovora argD* gene causes arginine auxotrophy, nonpathogenicity in apples, and reduced virulence in pears. *Applied and Environmental Microbiology*, 80, 6739–6749.

Raymundo, A. & Ries, S. (1980) Motility of *Erwinia amylovora*. *Phytopathology*, 70, 1062–1065.

Rogers, P.A., Eide, L., Klungland, A. & Ding, H. (2003) Reversible inactivation of *E. coli* endonuclease III via modification of its [4Fe-4S] cluster by nitric oxide. *DNA Repair*, 2, 809–817.

Santander, R.D. & Biosca, E.G. (2017) *Erwinia amylovora* psychrotrophic adaptations: evidence of pathogenic potential and survival at temperate and low environmental temperatures. *PeerJ*, 5, e3931.

Santander, R.D., Figàs-Segura, À. & Biosca, E.G. (2018) *Erwinia amylovora* catalases KatA and KatG are virulence factors and delay the starvation-induced viable but non-culturable (VBNC) response. *Molecular Plant Pathology*, 19, 922–934.

Schierle, C.F., Berkmen, M., Huber, D., Kumamoto, C., Boyd, D. & Beckwith, J. (2003) The DsbA signal sequence directs efficient, cotranslational export of passenger proteins to the *Escherichia coli* periplasm via the signal recognition particle pathway. *Journal of Bacteriology*, 185, 5706–5713.

Schwartz, C.J., Djaman, O., Imlay, J.A. & Kiley, P.J. (2000) The cysteine desulfurase, IscS, has a major role in in vivo Fe-S cluster formation in *Escherichia coli*. *Proceedings of the National Academy of Sciences of the United States of America*, 97, 9009–9014.

Sebaihia, M., Bocsanczy, A., Biehl, B., Quail, M., Perna, N., Glasner, J. et al. (2010) Complete genome sequence of the plant pathogen *Erwinia amylovora* strain ATCC 49946. *Journal of Bacteriology*, 192, 2020–2021.

Slack, S.M., Schachterle, J.K., Sweeney, E.M., Kharadi, R.R., Peng, J., Botti-Marino, M. et al. (2022) In-orchard population dynamics of *Erwinia amylovora* on apple flower stigmas. *Phytopathology*. https://doi.org/10.1094/PHYTO-01-21-0018-R

Slack, S.M., Zeng, Q., Outwater, C.A. & Sundin, G.W. (2017) Microbiological examination of *Erwinia amylovora* exopolysaccharide ooze. *Phytopathology*, 107, 403–411.

Takahashi, Y. & Nakamura, M. (1999) Functional assignment of the ORF2-*iscS-iscU-iscA-hscB-hscA-fdx*-ORF3 gene cluster involved in the assembly of Fe-S clusters in *Escherichia coli*. *Journal of Biochemistry*, 126, 917–926.

Tóth, E.N., Szabó, L.G., Botz, L. & Orosz-Kovács, Z. (2003) Effect of rootstocks on floral nectar composition in apple cultivars. *Plant Systematics and Evolution*, 238, 43–55.

Urbina, H.D., Silberg, J.J., Hoff, K.G. & Vickery, L.E. (2001) Transfer of sulfur from IscS to IscU during Fe/S cluster assembly. *Journal of Biological Chemistry*, 276, 44521–44526.

Wang, D., Clough, S.J., Zhao, Y., Korban, S., Sundin, G. & Toth, I. (2010) Regulatory genes and environmental regulation of amylovoran biosynthesis in *Erwinia amylovora*. *Acta Horticulturae*, 896, 195–202.

Wang, D., Korban, S.S. & Zhao, Y. (2009) The Rcs phosphorelay system is essential for pathogenicity in *Erwinia amylovora*. *Molecular Plant Pathology*, 10, 277–290.

Wei, Z.-M., Laby, R.J., Zumoff, C.H., Bauer, D.W., He, S.Y., Collmer, A. et al. (1992) Harpin, elicitor of the hypersensitive response produced by the plant pathogen *Erwinia amylovora*. *Science*, 257, 85–88.

Wunderlich, M. & Glockshuber, R. (1993) Redox properties of protein disulfide isomerase (DsbA) from *Escherichia coli*. *Protein Science*, 2, 717–726.

Yang, W., Rogers, P.A. & Ding, H. (2002) Repair of nitric oxide-modified ferredoxin [2Fe-2S] cluster by cysteine desulfurase (IscS). *Journal of Biological Chemistry*, 277, 12868–12873.

Yuan, X., McGhee, G.C., Slack, S.M. & Sundin, G.W. (2021) A novel signaling pathway connects thiamine biosynthesis, bacterial respiration, and production of the exopolysaccharide amylovoran in *Erwinia amylovora*. *Molecular Plant-Microbe Interactions*, 34, 1193–1208.

Zeng, Q., Mcnally, R.R. & Sundin, G.W. (2013) Global small RNA chaperone Hfq and regulatory small RNAs control virulence in the fire blight pathogen *Erwinia amylovora*. *Journal of Bacteriology*, 195, 1706–1717.

Zeng, Q. & Sundin, G.W. (2014) Genome-wide identification of Hfq-regulated small RNAs in the fire blight pathogen *Erwinia amylovora* discovered small RNAs with virulence regulatory function. *BMC Genomics*, 15, 414.

Zhao, Y., Blumer, S.E. & Sundin, G.W. (2005) Identification of *Erwinia amylovora* genes induced during infection of immature pear tissue. *Journal of Bacteriology*, 187, 8088–8103.

Zhao, Y., Qi, M. & Wang, D. (2010) Evolution and function of flagellar and non-flagellar type III secretion systems in *Erwinia amylovora*. *Acta Horticulturae*, 896, 177–184.

Zhao, Y., Wang, D., Nakka, S., Sundin, G. & Korbans, S. (2009) Systems level analysis of two-component signal transduction systems in *Erwinia amylovora*: role in virulence, regulation of amylovoran biosynthesis and swarming motility. *BMC Genomics*, 10, 245.

SUPPORTING INFORMATION

Additional supporting information may be found in the online version of the article at the publisher's website.

How to cite this article: Schachterle, J.K., Gdanetz, K., Pandya, I. & Sundin, G.W. (2022) Identification of novel virulence factors in *Erwinia amylovora* through temporal transcriptomic analysis of infected apple flowers under field conditions. *Molecular Plant Pathology*, 23, 855–869. https://doi.org/10.1111/mpp.13199